Coulomb Expansion of Laser-Excited Ion Plasmas

D. Feldbaum, N.V. Morrow, S. K. Dutta, and G. Raithel

FOCUS Center, Physics Department, University of Michigan, 500 East University, Ann Arbor, Michigan 48109-1120

(Received 12 March 2002; published 8 October 2002)

We determine the electric field in mm-sized clouds of cold Rb^+ ions, produced by photoionization of laser-cooled ^{87}Rb atoms in a magneto-optical trap, using the Stark effect of embedded Rydberg atoms. The dependence of the electric field on the time delay between the ion plasma production and the probe of the electric field reflects the Coulomb expansion of the plasma. Our experiments and models show expansion times $<1\mu$s.

DOI: 10.1103/PhysRevLett.89.173004 PACS numbers: 32.80.Pj, 32.60.+i, 52.20.–j

Cold plasmas generated by the laser excitation of laser-cooled clouds of atoms [1] have revealed novel phenomena, including recombination into Rydberg states [2,3] and plasma oscillations [4,5]. Dense clouds of Rydberg atoms have been found to evolve into cold plasmas [6] or, at lower density, to undergo a conversion into long-lived Rydberg states due to l mixing [7]. Wigner crystallization of ions in quasineutral cold plasmas confined in traps appears possible [8–10]. Very recently, the early evolution of neutral cold plasmas has been studied in simulations [11–13]. Rydberg atom spectroscopy is well suited to the study of plasma electric fields [14]. In the present paper, we employ this method to measure the Coulomb expansion of photoexcited, mm-sized plasmas consisting mostly of cold Rb^+ ions. We find, in agreement with a simple theoretical model, that these plasmas dissipate within 1 μs.

In our experiment [15], we obtain cold Rb^+ ion plasmas in a two-step optical excitation process. Laser-cooled ^{87}Rb atoms confined in a volume ≈ 1 mm^3 are excited from the ground state $5S_{1/2}$ to the $5P_{3/2}$ state using a diode laser pulse that strongly saturates the transition. A UV laser pulse ($\lambda_{UV} = 355$ nm, duration <10 ns, pulse energy $\lesssim 1$ mJ, fluence $\lesssim 5 \times 10^{16}$ cm^{-2}) partially ionizes the $5P_{3/2}$ atoms (ionization cross section $\approx 8 \times 10^{-18}$ cm^2), producing photoelectrons with 0.9 eV initial kinetic energy. These photoelectrons escape on a time scale of a few ns, leaving behind a cloud of slow Rb^+ ions. Both laser beams used for the photoionization are large enough in diameter to cover the entire atom cloud. Therefore, the initial ion probability distribution equals that of the atom cloud, and has been determined by absorptive CCD imaging of the atom cloud [15].

We probe the electric field in the expanding plasma as follows. At a time delay of 25 to 1000 ns after the UV pulse and while the lower-step laser is still on, $5P_{3/2}$ atoms embedded in the ion plasma are excited by a blue dye laser pulse ($\lambda \approx 480$ nm, duration <10 ns, bandwidth ≈ 10 GHz). The blue pulse excites bound Rydberg atoms, which subsequently undergo l mixing and slow thermal ionization [7]. The thermal electrons are counted using a microchannel plate detector and a photon counter, and the counts are recorded vs the wavelength of the blue laser. The Stark effect visible in the Rydberg excitation spectra is used to determine the plasma electric fields.

Figure 1 shows a typical experimental Rydberg excitation spectrum of atoms in an electric-field-bearing plasma. Electric-field-induced mixing of Rydberg states causes what appears as parity-forbidden transitions in Fig. 1: p lines and high-$\langle l \rangle$ states (states with near-zero quantum defects, labeled h) are observed to become increasingly prominent with increasing principal quantum number n. The electric field E causes the high-$\langle l \rangle$ states to fan out over an energy range $3n^2E$ (atomic units) ([16] and Fig. 2). Because of line broadening, the high-$\langle l \rangle$ states in Fig. 1 are not resolved into individual spectral lines but appear as the quasicontinuous spectral h features. The h features first show up as triangular structures between neighboring s and p lines and, with increasing n, progressively expand and fill in the spectral gaps of originally zero signal between the discrete s, p, and d states, which have large quantum defects ($\delta_s = 3.13$, $\delta_p = 2.65$, and $\delta_d = 1.34$). There are three types of spectral gaps, which we label hs-, mid- and pd-gaps. With decreasing

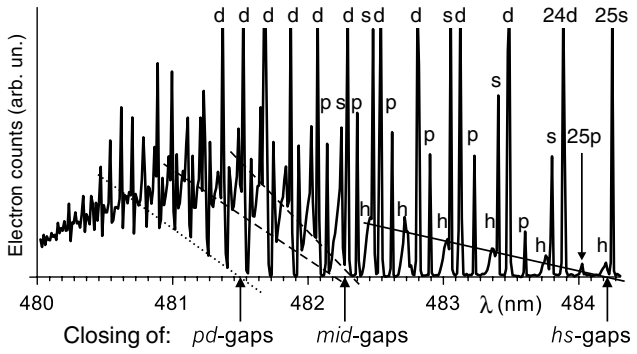

FIG. 1. Experimental Rydberg excitation spectrum of ^{87}Rb $5P_{3/2}$ atoms embedded in a laser-generated ion plasma. Three types of spectral ranges with low signal, denoted hs-, mid- and pd-gaps, become filled in at critical wavelengths that depend on the strength of the plasma electric field. The figure shows the construction that we use to determine the critical wavelengths at which the spectral gaps close.

 © 2002 The American Physical Society

wavelength, the gaps become filled in with significant signal in exactly that order, at well-defined critical wavelengths. Those wavelengths can be readily converted into critical effective quantum numbers n_{hs}, n_{mid}, and n_{pd}. We find that the n_i are robust indicators for the electric field, because they are solely determined by the general spreading behavior of the quasicontinuous h features and are only weakly affected by the power and frequency fluctuations of our Rydberg excitation laser.

Using the numerical parameters given in Fig. 2, which reflect the noninteger parts of the quantum defects of Rb and the linear Stark effect of the high-$\langle l \rangle$ states, the critical quantum numbers n_i at which the spectral gaps become filled in can be related to E as follows:

$$E = 0.086 n_{hs}^{-5} \qquad E = 0.23 n_{mid}^{-5}$$
$$E = 0.33 n_{pd}^{-5} \ \text{(atomic units)}. \tag{1}$$

Atoms other than Rb would follow similar relations with different numerical factors, dependent on their quantum defects. Equations (1) share the n^{-5} dependence of the well-known Inglis-Teller relation [17]. Equations (1) apply to Rydberg atom spectra in constant electric fields. In a plasma, the electric field typically follows probability distributions centered about a most probable electric field, and Eqs. (1) can be used to approximately determine that field.

We have measured a series of spectra for different delay times of the UV and blue laser pulses, shown in Fig. 3. The plasma-field-induced signatures recede to higher n as the delay time increases. This observation reflects the expansion of the ion plasma and the associated decrease of the plasma electric field. In Fig. 3, we determine the critical wavelengths at which the three types of spectral gaps (discussed above) close. The corresponding electric fields, obtained from Eqs. (1), depend on the pulse delay time as shown in Fig. 4 and demonstrate that the plasma dissipates within a time <1 μs. The electric-field decay time is much shorter than the dissipation time of quasineutral ultracold plasmas, which is of order 50 μs [1]. The measurements of the plasma electric field and its decay behavior are the main results of this paper.

We begin our discussion with the initial state of the plasma. Since the excitation beams are larger than the atom cloud, we assume that the plasma has an initial shape similar to that of the atom cloud. The area density distribution of the atom cloud used for the data shown in Fig. 3 is elliptical, with initial FWHM in the direction of the long and short axes of 2.0 ± 0.1 mm and 1.2 ± 0.1 mm, respectively. Using absorption images and magneto-optical-trap fluorescence measurements before and after the ionizing UV pulses, we estimate an ion number of 5.0×10^6 with a statistical uncertainty of 0.5×10^6.

The question arises whether there is a significant electron component present during the early stages of the plasma expansion. Using the kinetic energy of the photoexcited electrons, $\Delta E = 0.9$ eV, and the size of the atom cloud, an expression given in Ref. [1] can be used to estimate a critical number N^* of ions above which the space-charge effect of the ions becomes large enough to retain electrons in the ion cloud: $N^* = \Delta E\{\sqrt{2/\pi}e^2/(4\pi\epsilon_0\sigma)\}^{-1}$, where σ is the rms radius of the ion cloud.

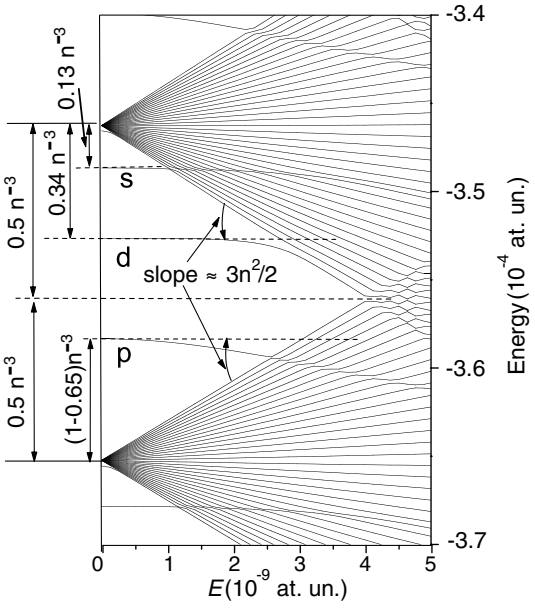

FIG. 2. Calculated Stark map of Rb in the vicinity of $n = 29$ and $n = 30$.

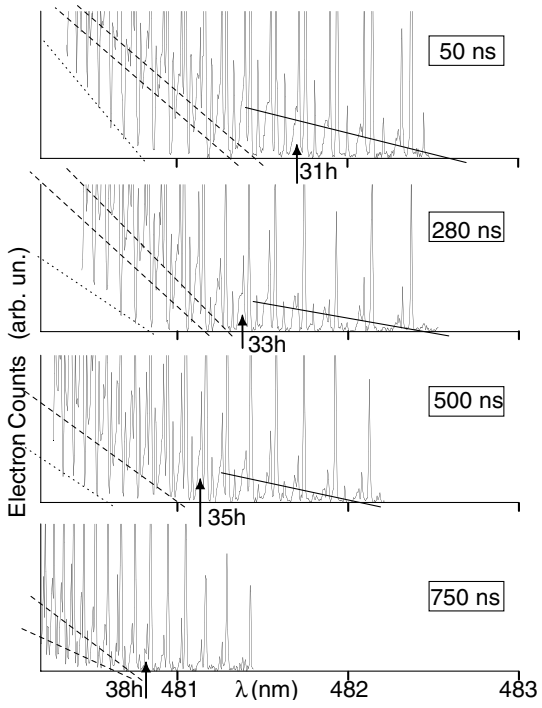

FIG. 3. Experimental Rydberg excitation spectra of ^{87}Rb $5P_{3/2}$ atoms embedded in photoexcited plasmas. The delay times between the plasma excitation and the excitation of Rydberg atoms are indicated. The lines indicate the closing of the pd- (dotted), mid- (dashed), and hs-gaps (solid).

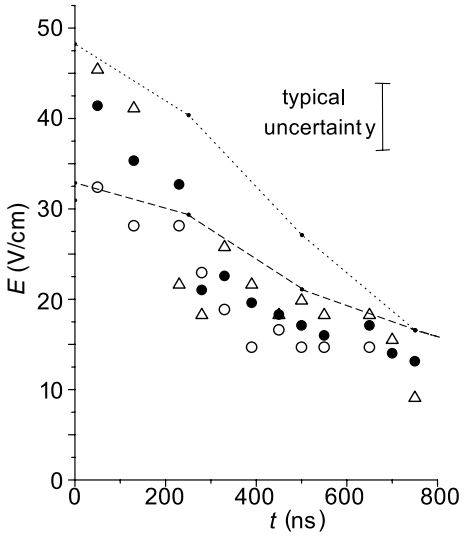

FIG. 4. Time dependence of the electric field in photoexcited plasmas obtained from the closing of the pd- (triangles), mid- (full circles) and hs-gaps (open circles) observed in experimental Rydberg excitation spectra. The indicated typical uncertainty is due to the graphical determination of the wavelengths at which the spectral gaps close. The lines show theoretical electric fields derived from a model explained in the text.

With an increasing fraction of retained electrons the plasma becomes increasingly neutral. As a result, beyond a critical number of ions the electric-field-induced signatures in the Rydberg atom excitation spectra recede, indicating the collection of electrons in the plasma that neutralize the macroscopic plasma electric field. In earlier work we have observed and pointed out this effect [18]. In our present work, we aim for a large initial electric field. Therefore, we keep the ion number low enough that the electric-field-induced signatures in the spectra are not diminished. Thus, we are confident that the fraction of retained electrons is zero or very small. A moderate inconsistency between the above quoted equation for N^* and the estimated ion number and cloud size may be due to the deviations of our ion cloud from a spherical Gaussian and/or to systematic errors in the determination of the ion number.

To model the plasma expansion, we consider the plasma a one-component "charged liquid" with a slowly varying, spherically symmetric density distribution and constant charge/mass ratio. This model applies only if there are no electrons in the plasma; if there were, more sophisticated models [11–13] would have to be used. The expansion is simulated using a set of 2000 concentric shells evenly covered with charges consistent with the initial charge distribution, which is assumed to be a Gaussian $g(r)$ with a FWHM diameter of 1.65 mm. As Fig. 5(a) shows, the charge distribution does not preserve its shape during the expansion. In the central region, the charge density drops and tends to become constant over a large volume, while at the perimeter of the expanding

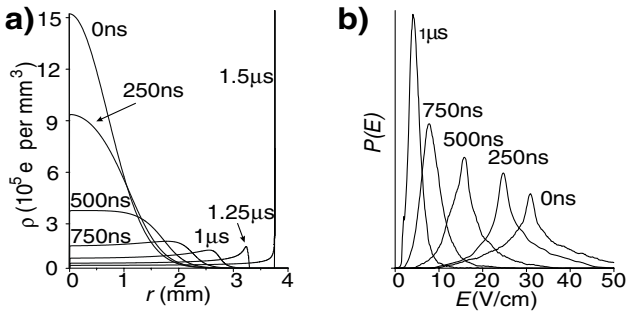

FIG. 5. (a) Calculated radial dependence of the charge density ρ at the indicated times for an initially Gaussian ion cloud. The corresponding probability distributions for the detected electric field, shown in (b), include the effect of microfields (see text).

cloud a relatively strongly charged outer layer develops. At times later than about 1.5 μs, the charge density of the outer layer becomes singular, forming an expanding shock front. We believe that a model developed by Robicheaux *et al.* [12] will, in the limit of a high initial electron energy and a large initial electron escape probability, produce results consistent with ours.

The probability distribution $P(E)$ for the electric field experienced by an atom randomly placed in the plasma is determined as follows. The distributions of Fig. 5(a) are used to randomly place a set of discrete ions. The $5P_{3/2}$-detector atoms are placed according to the same function $g(r)$ that is also used for the initial ion distribution. This placement of the detector atoms is justified by the fact that the ion and Rydberg atom excitation processes are not saturated and the cloud of $5S_{1/2}$ and $5P_{3/2}$ atoms does not expand during the time delay between the UV and the blue pulses (unlike the rapidly expanding ion plasma). In the described procedure, the electric-field sampling over the plasma volume is weighted by $g(r)$, and it accounts for microfield effects [19]. The resultant distributions $P(E)$ are shown in Fig. 5(b), and the corresponding field averages $\int P(E)EdE$ are shown as dashed curve in Fig. 4.

We have estimated the uncertainty inherent to the analysis scheme used for the experimental data. For about 50 field values we have calculated Rydberg atom excitation spectra for random atomic orientation and light polarization (methods described in [20]). To account for the laser linewidth, the spectra are convoluted with a Gaussian of 10 GHz FWHM, yielding spectra $S(E, \lambda)$. Then, the probability distributions $P(E)$ shown in Fig. 5(b) are used to form a weighted sum $S(\lambda)$ of the $S(E, \lambda)$. The $S(\lambda)$ show excellent qualitative agreement with the measured spectra (compare Figs. 3 and 6). We have then used the graphical method to identify the critical wavelengths, explained in Fig. 1, and Eqs. (1) to extract electric-field values from the spectra $S(\lambda)$. Those fields are shown as dotted line in Fig. 4.

Our model qualitatively reproduces the experimentally observed electric-field decay behavior. The values of

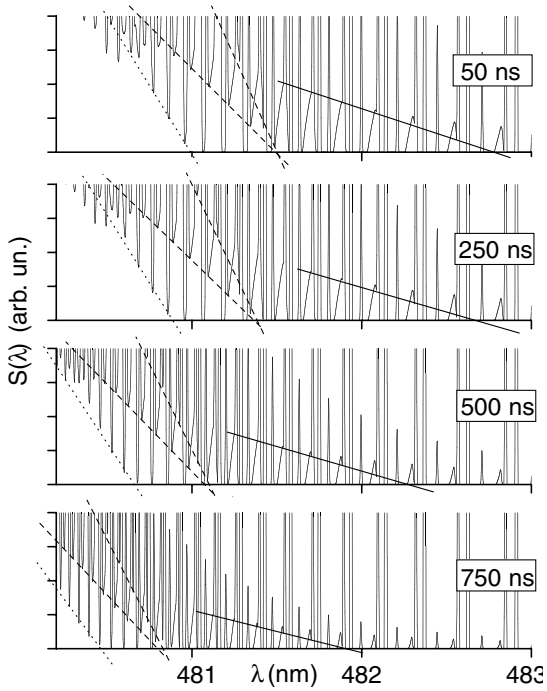

FIG. 6. Calculated isotropic excitation spectra $S(\lambda)$ of a Gaussian cloud of ^{87}Rb $5P$ atoms into Rydberg states in the presence of 5×10^6 discrete Rb^+ ions with spatial distributions shown in Fig. 5(a).

experimental and theoretical electric fields agree to within about 40%. Since a number of difficult calibration measurements (cloud size, atom number, photoionization probability) had to be performed in order to arrive at a quantitative experiment-theory comparison, this level of agreement appears satisfactory. A comparison of the data shown in Fig. 4 with additional calculations in which the effect of the microfields on $P(E)$ was ignored has further shown that, at present, we are not able to isolate microfield and other local effects of the charge carrier distribution. The short expansion time of non-neutral plasmas is, obviously, a result of the strong Coulomb repulsion between the ions. In contrast, quasineutral ultracold plasmas expand mostly due to the pressure of the electron component [1,12]; that mechanism leads to a much slower plasma expansion. We expect that, when the fraction of electrons retained in the plasma is increased from 0% to 100%, there is a gradual transition between a Coulomb expansion and a pressure-driven expansion. The model in [12] should be suited to theoretically study these issues, while position- and time-resolved electric-field measurements of the plasma could provide experimental insight.

In summary, we have used spectroscopic electric-field measurements and numerical models to study the expansion of an ultracold non-neutral plasma of Rb^+ ions. We have found agreement in observed and calculated expansion times. The developed field measurement method has considerable potential. In future experiments, we plan position-sensitive electric-field measurement using crossed and focused Rydberg atom excitation beams. The use of a laser with a narrow bandwidth (~ 1 MHz $= 1/10\,000$ of our current spectral resolution) will allow us to measure electric-field distributions rather than average fields. It should thus become possible to isolate the effect of the microfields and to measure the Holtsmark distribution [21]. Accurate field measurements could also reveal inhomogeneities and instabilities in the expanding plasma. A study of the shock front dynamics mentioned in the paper should also be possible. Spatial order in the charge carrier arrangement, such as Wigner crystals [8], may become detectable via measurements of electric-field distributions.

We acknowledge support by the NSF (Grants No. PHY-9875553 and No. PHY-0114336), and partial support by the Chemical Sciences, Geosciences and Biosciences Division of the Office of Basic Energy Sciences, Office of Science, U.S. Department of Energy. We thank Professor P. Bucksbaum for inspiring discussions and generous loaning of equipment, and Dr. B. K. Teo for assistance.

[1] T. C. Killian *et al.*, Phys. Rev. Lett. **83**, 4776 (1999).
[2] T. C. Killian *et al.*, Phys. Rev. Lett. **86**, 3759 (2000).
[3] Y. Hahn, Phys. Lett. A **231**, 82 (1997).
[4] D. H. E. Dubin and J. P. Schiffer, Phys. Rev. E **53**, 5249 (1996).
[5] S. Kulin *et al.*, Phys. Rev. Lett. **85**, 318 (2000).
[6] M. P. Robinson *et al.*, Phys. Rev. Lett. **85**, 4466 (2000).
[7] S. Dutta *et al.*, Phys. Rev. Lett. **86**, 3993 (2001).
[8] S. Ichimaru, Rev. Mod. Phys. **54**, 1017 (1982).
[9] A. P. Gavrilyuk *et al.*, Russ. Phys. J. **42**, 744 (1999), and references therein.
[10] Y. Hahn, Phys. Rev. E **64**, 046409 (2001).
[11] S. Mazevet *et al.*, Phys. Rev. Lett. **88**, 55001 (2002).
[12] F. Robicheaux and J. D. Hanson, Phys. Rev. Lett. **88**, 55002 (2002).
[13] S. G. Kuzmin and T. M. O'Neil, Phys. Rev. Lett. **88**, 65003 (2002).
[14] B. N. Ganguly, J. Appl. Phys. **61**, 571 (1986); J. R. Shoemaker *et al.*, Appl. Phys. Lett. **52**, 2019 (1988); G. A. Hebner *et al.*, J. Appl. Phys. **76**, 4036 (1994).
[15] D. Feldbaum *et al.*, in *Non-Neutral Plasma Physics IV*, edited by F. Anderegg, L. Schweikhard, and C. F. Driscoll, AIP Conf. Proc. No. 606 (AIP, New York, 2002).
[16] T. F. Gallagher, *Rydberg Atoms* (Cambridge University Press, Cambridge, United Kingdom, 1994).
[17] D. R. Inglis and E. Teller, J. Astrophys. **90**, 439 (1939).
[18] S. K. Dutta, D. Feldbaum, and G. Raithel, e-print physics/0007004 (2000).
[19] It is beyond the scope of this paper to analyze the effect of the microfields on the expansion dynamics of the plasma.
[20] M. L. Zimmerman *et al.*, Phys. Rev. A **20**, 2251 (1979).
[21] S. Chandrasekhar, in *Selected Papers on Noise and Stochastic Processes*, edited by N. Wax (Dover, New York, 1954).